JOURNAL OF GEOPHYSICAL RESEARCH, VOL. 102, NO. A12, PAGES 26,919-26,926, DECEMBER 1, 1997

Contribution of obliquely incident particles to neutron monitor counting rate

J. M. Clem, J. W. Bieber and P. Evenson

Bartol Research Institute, University of Delaware, Newark

D. Hall and J. E. Humble

Department of Physics, University of Tasmania, Hobart, Tasmania, Australia

M. Duldig

Australian Antarctic Division, Kingston, Tasmania, Australia

Abstract. We describe a new method for calculating geomagnetic cutoffs that incorporates obliquely incident primaries, and we use it to interpret a sea level neutron monitor latitude survey. Effects due to obliquely incident primaries are significant and may be responsible for anomalies observed in this and other latitude surveys. We define an "apparent" cutoff that takes these obliquely incident particles into account. Use of our apparent cutoff in a Dorman function fit to the 1994-1995 Bartol Research Institute–University of Tasmania latitude survey data results in a significant improvement over use of the more conventional effective vertical cutoff.

1. Introduction

Analysis of neutron monitor data typically requires knowledge of the geomagnetic cutoff [*Shea et al.,* 1965; *Cooke et al.,* 1991] since the geomagnetic field and magnetosphere impose a lower limit on the energy of primary cosmic rays that enter the atmosphere. Primary particles admitted by the magnetic field propagate through the atmosphere and undergo multiple interactions, ultimately producing cascades of secondary particles detected by ground based neutron monitors. In a neutron monitor, BF_3 (boron trifluoride) proportional counters surrounded by a lead target detect thermal neutrons produced locally by interacting incident neutrons, protons, pions, and muons. These have relative contributions to the counting rate of roughly 85%, 7%, 1%, and 6% [*Hatton,* 1971] respectively. The total counting rate observed is thus directly related to the primary flux, but complete interpretation of the data requires knowledge of detector response, atmospheric particle transport, primary energy spectrum, and geomagnetic cutoff rigidity. In this paper we focus specifically on the proper definition of the cutoff.

For many purposes the effective vertical cutoff (i.e., the cutoff for a vertically incident particle) is sufficient, but, in reality, the effective cutoff rigidity depends upon the details of the cosmic ray penumbra in each possible direction of incidence [*Cooke et al.,* 1991]. Since cosmic rays arrive almost isotropically, there is a large population of obliquely incident primaries. Although atmospheric absorption increases rapidly with increasing slant depth, and a good first approximation is to consider only the particles incident vertically, response to off-vertical particles is finite, and the primary incidence direction does not determine the slant depth for all secondary components. In fact, scattering from multiple inelastic interactions removes some memory of the primary incidence direction from hadronic daughter particles at ground level. This reduces the attenuation of obliquely incident particles relative to that which would occur if an oblique path were followed all the way to the ground.

A neutron monitor latitude survey is conducted with a mobile detector that records counting rates during passage across a range of geomagnetic cutoffs [*Moraal et al.,* 1989, and references therein]. The scientific motivation behind such a survey is three fold: to improve knowledge of geomagnetic cutoffs; to study the primary cosmic ray spectrum; and to understand the neutron monitor energy response function. Equation (1) provides a mathematical description of the relationship between parameters relevant to a latitude survey in the usual approximation:

$$N(P_C) = \int_{P_C}^{\infty} S(P) j(P) dP. \qquad (1)$$

$N(P_C)$ is the neutron monitor counting rate, P_C is the

Copyright 1997 by the American Geophysical Union.

Paper number 97JA02366.
0148-0227/97/97JA-02366$09.00

geomagnetic cutoff, $S(P)$ is the neutron monitor yield function, and $j(P)$ is the primary cosmic ray spectrum.

Figure 1 displays a course plot of the latitude survey conducted from December 1994 to April 1995 by the Bartol Research Institute and the University of Tasmania on board the U.S. Coast Guard icebreaker *Polar Star*. Annotated effective vertical cutoffs show the part of the survey considered in this paper. Figure 2 shows the data taken during this part of the survey, together with a least squares fit of a Dorman function [*Dorman et al.*, 1970] to the counting rates. These data are corrected to a standard pressure of 760 mm Hg using a pressure coefficient that varies with cutoff rigidity as

$$\alpha = 0.983515 - 0.00698286 P_c \,, \qquad (2)$$

where α is pressure coefficient in units of percent per millimeter Hg and P_c is geomagnetic cutoff in units of GV (gigavolts). Equation (2) was derived empirically from a fit to pressure coefficients reported by 11 neutron monitor stations near sea level with various cutoffs. To reduce effects of time variations of the overall cosmic ray intensity, the data were also normalized to the count rate measured by the McMurdo neutron monitor. Specifically, the count rate of the survey instrument at time t was multiplied by $M(t_0)/M(t)$, where M represents the McMurdo rate and t_0 is a reference time defined as the hour from 1200 to 1300 UT on March 8, 1995.

The result is typical of prior surveys, showing deviations at the 0.6% level, which is about a factor of 2 larger than would result from counting statistics alone. Many of the deviations have a random appearance, but others are highly systematic, such as in the region from 6 to 8 GV that we refer to as the "hump". *Stoker* [1995] noted similar humps in airborne surveys and suggested that obliquely incident particles may be responsible [*Rao et al.*, 1963]. In order to quantify the effects of obliquely incident primaries, we have developed the concept of "apparent" cutoff, which includes these effects, the variation of cutoff with direction of incidence, and propagation of the secondary particles through the atmosphere.

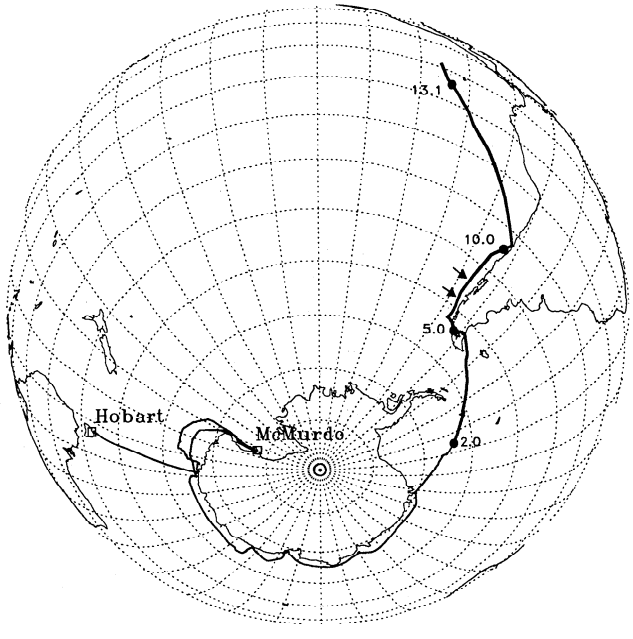

Figure 1. Course plot of 1994-1995 Bartol/Tasmania latitude survey. The appropriate portion of the survey is annotated with calculated effective vertical cutoffs. The arrows indicate the associated locations of the example cutoff sky maps shown in Figures 4 and 5.

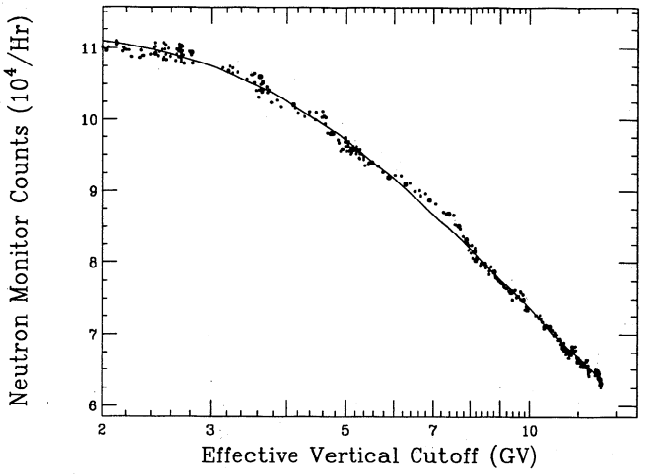

Figure 2. Count rate recorded during the portion of the survey highlighted in Figure 1. The large dots indicate locations for which a cutoff sky map is calculated.

2. Apparent Cutoff

In this paper we compute cutoffs for specific directions of incidence using the effective cutoff approximation as defined by *Shea et al.* [1965] and *Cooke et al.* [1991]. Examining the validity of the effective cutoff approximation will be the subject of future work. We then adopt an operational definition of a quantity we term the apparent cutoff. We define the apparent cutoff as that rigidity which, if uniform over the whole sky, would yield the same neutron monitor counting rate as the real, angular dependent cutoff distribution.

The mathematical definition is

$$N = \int_{\text{sky}} d\Omega \int_{P_c(\Omega)}^{\infty} S(P,\Omega) j(P) dP,$$

$$\equiv \int_{\text{sky}} d\Omega \int_{P_{\text{apparent}}}^{\infty} S(P,\Omega) j(P) dP, \qquad (3)$$

where N is the counting rate, the first integral is over solid angle, and the second is over rigidity. In (3) we indicate explicitly that both the cutoff and the yield function depend on incident direction. $P_c(\Omega)$ is the geomagnetic cutoff at all zeniths and azimuths that we term a "cutoff sky map." The direction-dependent yield func-

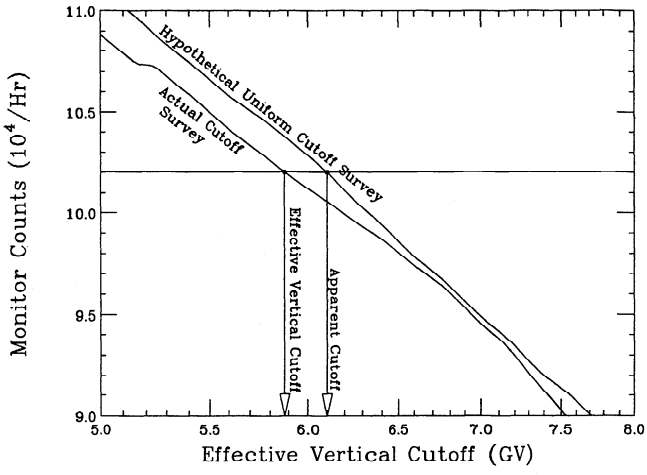

Figure 3. Graphical definition of the apparent cutoff based upon simulated count rates for locations in the actual survey, but in this context, used only to illustrate schematically the definition of the apparent cutoff.

tion $S(P,\Omega)$ appearing in (3) is different from the function $S(P)$ in (1), because $S(P)$ describes the yield integrated over all directions of incidence. In general, both types of yield function depend on atmospheric depth as well, but we are concerned only with sea level measurements in this paper. We assume for the remainder of the paper that the yield function $S(P,\Omega)$ only depends on incident zenith angle and is independent of incident azimuth. The lower integration limit P_{apparent} required to make the second form of the rigidity integral numerically equal to the first is the apparent cutoff.

A graphical definition of the apparent cutoff is displayed in Figure 3 where the top curve is the simulated result of a hypothetical survey in which the cutoff at each location is uniform over the sky and equals the effective vertical cutoff at that location. The bottom curve in Figure 3 is based upon the same simulation method (see section 4) but uses the actual cutoff sky map for locations along the ship course in Figure 1. The rigidity at which a horizontal line drawn through the "observed" counting rate (lower curve) at a given location intersects the hypothetical survey (upper curve) is, by definition, the apparent cutoff. In the rest of this paper we report the results of a calculation originally intended only to provide a good estimate of the difference between the apparent cutoff and the effective vertical cutoff. We summarize this calculation in some detail, as we have been pleasantly surprised at the accuracy with which it reproduces the whole survey in an absolute, not only differential, sense.

3. Cutoff Sky Maps

We define a sky map to be a systematic calculation of effective cutoff for different directions of incidence at a particular location. A sky map is calculated by tracing trajectories of charged particles through the geomagnetic field to determine allowed and forbidden rigidities [*Lin et al.*, 1995]. Figure 4 and Figure 5 provide two examples of cutoff sky maps. The solid curves represent isocutoff contours, the radial coordinate represents the zenith angle of incidence, and the angular coordinate represents the azimuthal direction of incidence, with incidence from the north at the top. The cutoff sky maps

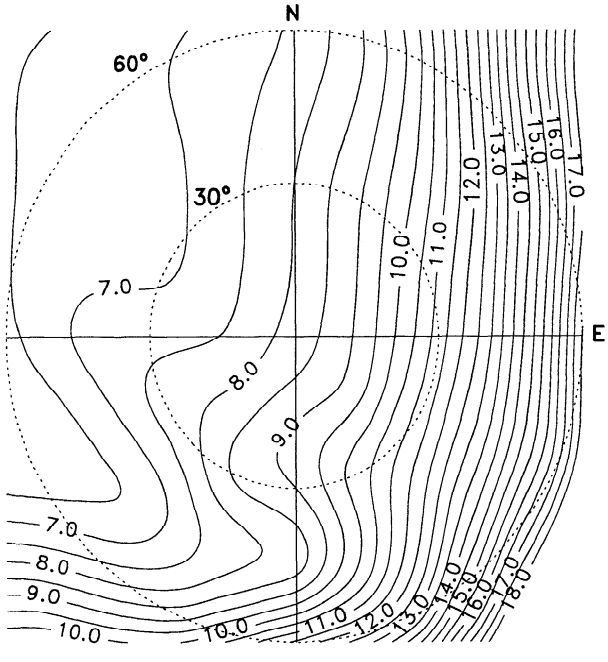

Figure 4. Example of an effective cutoff rigidity sky map for 43.92°S, 76.64°W (top arrow in Figure 1) at 2330 UT on day 75 of 1995. Here the effective vertical cutoff is 8.23 GV and the apparent cutoff is 8.65 GV.

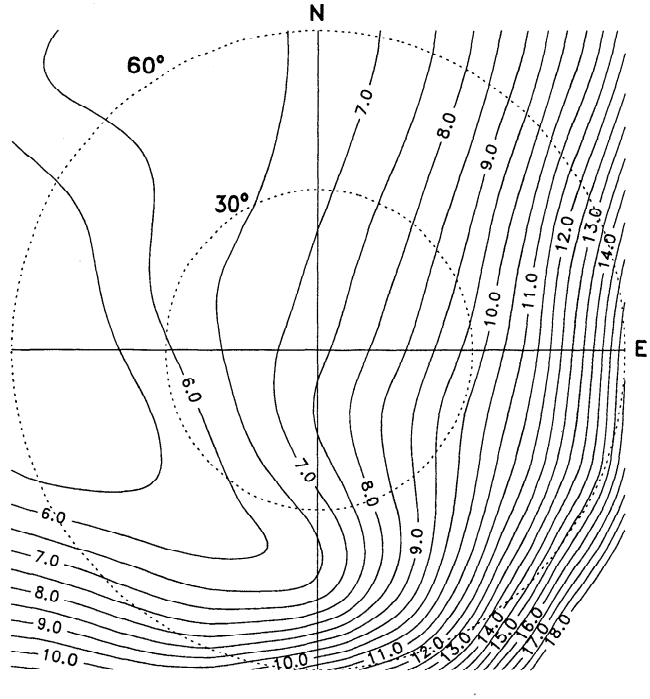

Figure 5. Example of an effective cutoff rigidity sky map for 48.19°S, 77.02°W (bottom arrow in Figure 1) at 0430 UT on day 75 of 1995. Here the effective vertical cutoff is 7.37 GV and the apparent cutoff is 7.38 GV.

exclude points with zenith angles greater than 75° since sea level yields are almost insignificant above this angle. As noted previously, at each point we calculate the *Shea et al.* [1965] and *Cooke et al.* [1991] effective cutoff.

The major characteristics of a sky map that affect the apparent cutoff are curvature of and gradients in the isocutoff contours. In Figure 4, curvature produces a structure in which cutoffs greater than the effective vertical cutoff occupy more than half the available solid angle near the zenith. It also has steeper gradients at higher cutoffs. Both effects tend to make the apparent cutoff higher than the effective vertical cutoff. Anticipating the calculation outlined below, the effective vertical cutoff is 8.23 GV while the apparent cutoff is 8.65 GV. Figure 5 shows a sky map with a a somewhat different structure in which curvature and gradient effects act in opposite directions. In this case the effective vertical cutoff is 7.37 GV while the apparent cutoff is 7.38 GV. If this were always the case, there would be no reason to consider anything but the effective vertical cutoff for calculations of the accuracy presented in this paper. As we shall see, however, the result obtained for Figure 4 is the more typical one.

4. Atmospheric Propagation

4.1. Method

We calculated propagation of primary particles through the Earth's atmosphere with the three-dimensional Monte Carlo transport program entitled fluctuating kascades (FLUKA) [*Fassó et al.*, 1997, 1995, 1994, 1993] maintained at Insituto Nazionale di Fisica Nucleare (INFN) in Milan, Italy. An initially isotropic distribution of primary particles is filtered through a sky map calculated for each geographical location, and the surviving particles are transported through the atmosphere. The simulated ground level particle intensities, folded with the NM-64 detector response [*Hatton*, 1971], are then used to calculate a geographically dependent NM-64 counting rate. The details of the simulation are described herein.

Primary protons and alphas are selected from a spectrum with power index in momentum of −2.7 [*Seo et al.*, 1991] solar modulated for the epoch of the survey ($\kappa_\circ = 94.34 \times 10^{20}$ cm^2/(s GV)). The modulated spectra were determined [*Beatty et al.*, 1993] by solving the Fokker-Planker equation for the spherically symmetric model of the interplanterary medium including diffusion, convection, and adiabatic deceleration. For practical reasons we limit the rigidity range to 0.75 — 2000GV which encompasses a total integrated nucleon flux of 1.2/(cm^2 s). The relative composition of particles entering the atmosphere was chosen as 85% protons and 15% alphas, while heavier cosmic rays were represented by multiple alphas. Alpha particles are initially transported with a separate package, HEAVY [*Engel et al.*, 1992] to simulate fragmentation. This package interfaces with FLUKA to provide interaction starting points (A. Ferrari, personal communication, 1997) for each nucleon originating from a helium nucleus.

The atmosphere is divided into sixty 2000 km diameter, flat, circular slabs with differing density to simulate the actual density profile [*Gaisser*, 1990] with a total column density of 1033 g/cm^2. Above 500 m the atmospheric composition [*Zombeck*, 1982] is constant with a 23.3% O_2, 75.4% N_2 and 1.3% Ar distribution by mass, while below 500 m a varying addition of H_2 from 0.06% at sea level to 0.01% at 500 m is included to account for the abundance of water vapor. The quantity of water vapor above 500 m is insignificant for these purposes.

The upper boundary is at a height of 65 km. A single 1 cm^2 element centered on the upper boundary is illuminated with primaries uniformly in $\cos^2(\theta)$ and in ϕ, where θ is the zenith angle of incidence and ϕ is the azimuth of incidence [*Sullivan*, 1971]. Particle intensity at sea level is determined by superimposing all 1 cm^2 elements on the bottom boundary. Owing to translational invariance, this process is equivalent to illuminating the entire sky and recording the flux in a single 1 cm^2 element at sea level, but it requires far less computer time.

An event database was accumulated from outputs of many runs with different random seeds. The information for all generated primaries and resulting particles at sea level was stored in a format such that the sea level particles could be linked to the parent primary. This format allows the same database to be used for calculations with different sky maps.

4.2. Comparison with Measured Muon, Proton and Neutron Fluxes

As a check, sea-level vertical particle fluxes [*Rossi*, 1948] are calculated from the event data base and com-

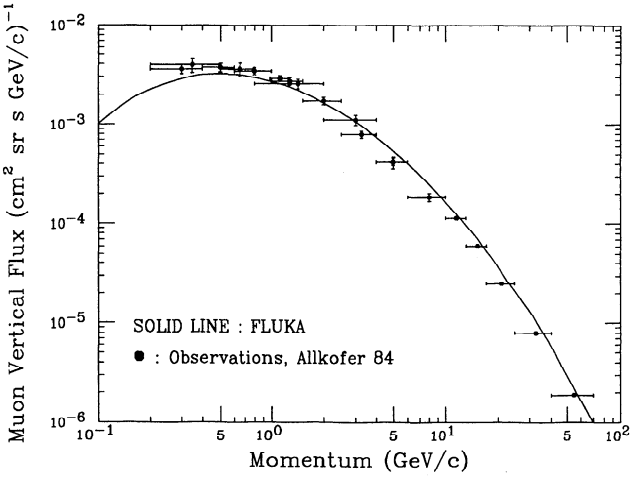

Figure 6. Sea level muon momentum vertical flux observations compared with the FLUKA simulation with 2.3GV uniform cutoff. Observations are from *Allkofer and Grieder* [1984].

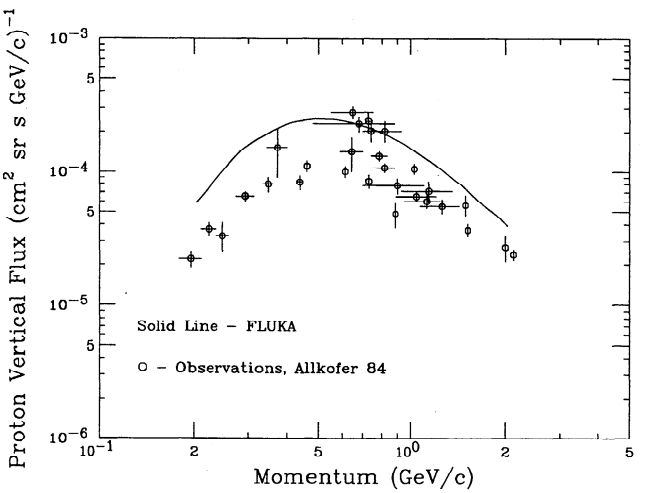

Figure 7. Sea level proton vertical flux observations compared with the FLUKA simulation with 4.5 GV uniform cutoff. Observations are from *Allkofer and Grieder* [1984].

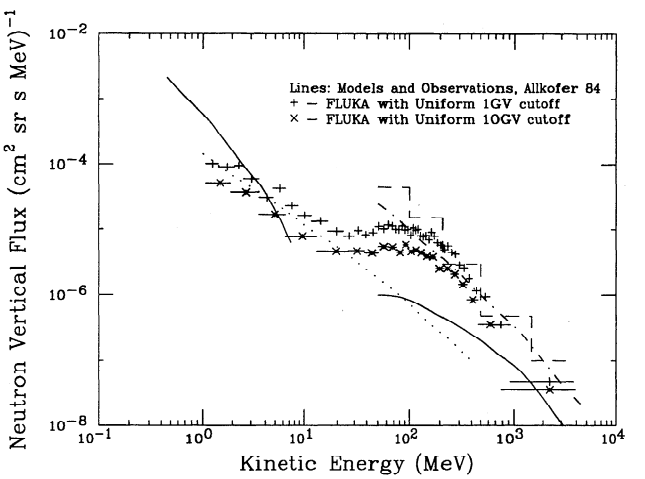

Figure 8. Sea level neutron vertical flux observations compared with the FLUKA simulation with 1GV and 10GV uniform cutoff.

pared to published data [*Allkofer and Grieder,* 1984]. The absolute normalization of the simulated flux is determined from the number of generated primaries with no free parameters in the comparison. The particle types tracked are muons, protons, and neutrons.

Muon vertical flux is shown in Figure 6, with the calculation performed for a uniform cutoff at 2.3 GV. This cutoff value is chosen since the majority of the observations [*Allkofer and Grieder,* 1984] displayed were made in Kiel, Germany, where the effective vertical cutoff is roughly 2.3GV. Observed and simulated muon data agree quite well.

Figure 7 compares simulated proton vertical fluxes with the observed values [*Allkofer and Grieder,* 1984] for a uniform cutoff at 4.5 GV appropriate for the observation site for most of the reported measurements (Berkeley, California). The simulated intensity is somewhat higher than the majority of observed data, which might be due to use of a solar modulation level that was different during observation time than for the simulated primary flux or to a steeper angular distribution from neglecting the Earth's curvature. Another possible systematic effect could be the result of using a uniform cutoff instead of an appropriate cutoff sky map.

In Figure 8 the simulated vertical neutron flux is compared with published measurements and models [*Allkofer and Grieder,* 1984]. Very few measurements of neutron spectra within the energy range of interest have been reported, and those that have are lacking in consistency. The structure in the simulated flux is probably due to the slow rise in the inelastic cross-sections with decreasing energy which peaks at 10 MeV and then steeply falls off. Below 10 MeV the total cross section is dominated by elastic interactions. Under the circumstances we can safely report that the simulation is not inconsistent with the displayed flux measurements and models.

4.3. Simulated Latitude Survey

To convert sea level particle intensities to a neutron monitor counting rate, one must know the detection efficiency of an NM-64 system. Using data from *Hatton* [1971] we determined the mean number of counts per incident secondary particle for a six-tube NM-64 detector as a function of incident angle, energy, and particle type. Since the survey monitor is a three-tube NM-64, a scale factor of 0.5 has been applied to the six-tube detection efficiency to account for the smaller monitor. The scale factor 0.5 is obviously not exact, because edge effects are more important in the smaller monitor, with observations suggesting a maximum 15 % systematic effect.

Cutoff sky maps for different locations on the survey are used to calculate the sea level neutron monitor counting rate by using the angle-dependent cutoff to select parent primaries from the event database. Particle fluxes at sea level are summed, and the count rate is determined by applying the detection efficiency to the sea level particle intensities. In Figure 9 the sim-

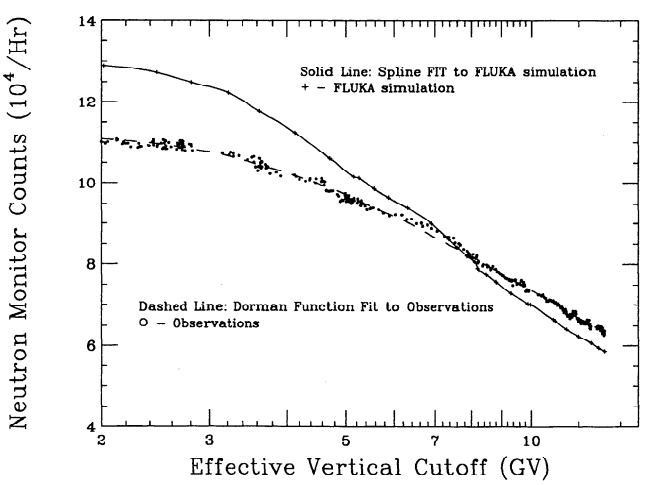

Figure 9. Simulated 1994-1995 latitude survey using FLUKA compared with the actual data displayed in Figure 2.

ulated counting rate is compared with observations as a function of effective vertical cutoff. We are somewhat surprised by how well this calculation agrees with the data in an absolute sense, and we are exploring the possibility of improving the calculation. However in the remainder of this paper we use this calculation only to estimate the deviation of the apparent cutoff from the effective vertical cutoff.

4.4. Neutron Monitor Angular Response

Figure 10 summarizes the propagation simulation in a manner that is convenient for calculation of apparent cutoffs. The horizontal axis is the cosine of the angle of incidence (with respect to the zenith) of a hypothetical unidirectional, uniform illumination of cosmic rays with our assumed spectral shape and composition and with a sharp cutoff at the indicated rigidity. The vertical axis is the rigidity integral that appears in (3), with the units of six-tube NM-64 counts per second per unit solid angle of incident primaries.

Empirically, when plotted against $\cos\theta$, straight semilog lines are an excellent approximation to the results of the full calculation. Thus we can approximate the integral over rigidity with the following relation:

$$\int_{P_c}^{\infty} S(P,\Omega)j(P)dP \approx \exp\left[A(P_c)\cos\theta + B(P_c)\right] \quad (4)$$

Fit parameters A and B for several different cutoff rigidities are given in Table 1.

It is interesting to note that the reduction in response with increasing angle of incidence is less rapid than predicted by an exponential relationship on $\sec(\theta)$ as would be expected from a simple attenuation model. The random deviations in particle trajectories from multiple inelastic collisions are significant enough to remove most of the correlation between the initial conditions of a primary trajectory and the total atmospheric path length of a daughter hadron at sea level. Such multiple interactions thus reduce the expected attenuation of the obliquely incident particles.

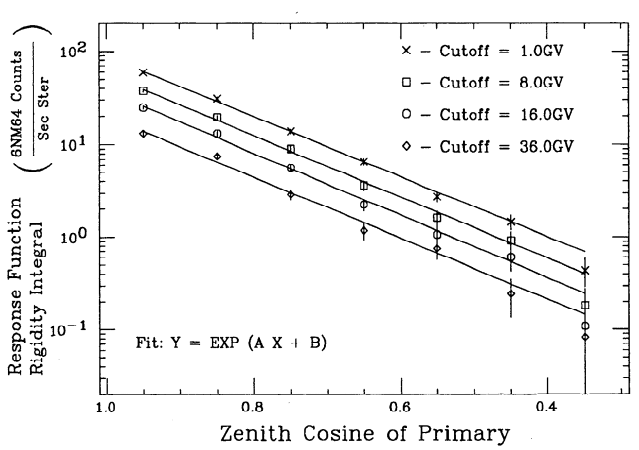

Figure 10. Calculated angular response of a six-tube neutron monitor NM-64.

Table 1. Angular Response Fit parameters

Cutoff Rigidity, GV	B	A
0	-2.9823	7.4698
1	-2.9835	7.4710
2	-3.0271	7.5080
4	-3.2037	7.5769
8	-3.5830	7.6308
12	-3.8877	7.6922
16	-4.1064	7.7447
20	-4.34467	7.84088
24	-4.47619	7.83255
28	-4.54340	7.76669
32	-4.55948	7.67227
36	-4.57373	7.58015

5. Effective Vertical and Apparent Cutoff Comparison

Calculation of a single cutoff sky map requires 3 to 4 days of CPU time on our Digital Equipment Corporation alpha workstation. Therefore to reduce computer time, only 30 locations on the latitude survey were chosen for a full calculation. Apparent cutoffs were determined from each sky map by simulating both cases in Figure 3 and interpreting the result as a correction to the calculated effective vertical cutoff. Resulting differences are plotted in Figure 11.

Figure 12 shows the observed data plotted against the calculated apparent cutoff, i.e., the effective vertical cutoff plus the correction from Figure 11. See Figure 2 for a plot of the same data against effective vertical cutoff. The fit to a Dorman function is significantly improved through near elimination of the hump.

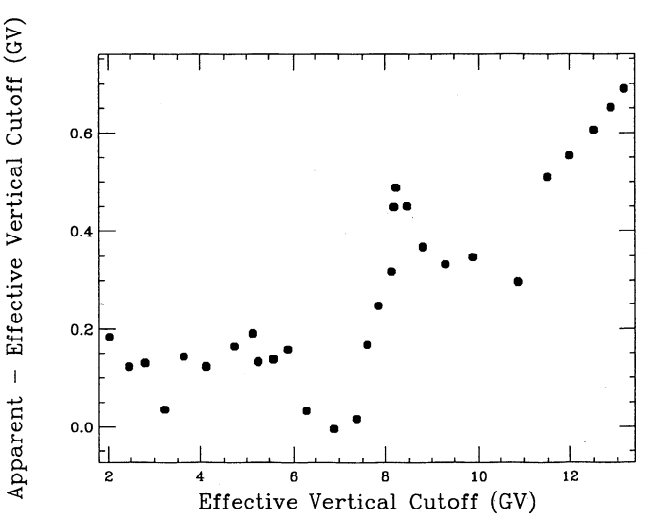

Figure 11. Deviation of apparent cutoff from effective vertical cutoff, as a function of effective vertical cutoff, for selected locations on the 1994-1995 survey.

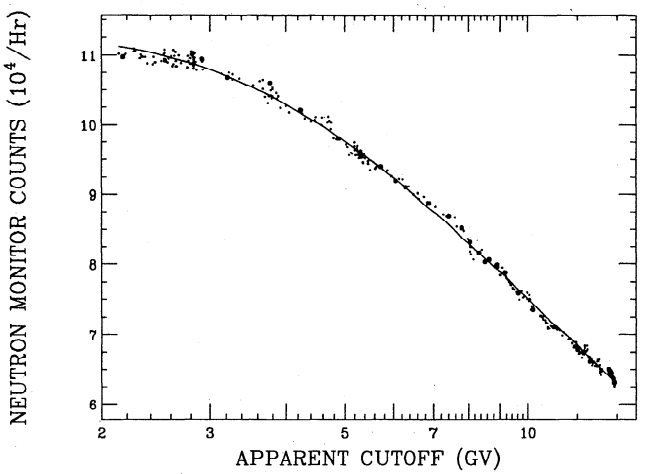

Figure 12. Observed neutron monitor counting rate versus apparent cutoff. Large dots show actual calculations; small dots show interpolated values.

It is curious (see Figure 11) that the hump originates from a region where the effective vertical cutoff is an unusually good approximation to the apparent cutoff. Our analysis indicates that the effective vertical cutoff is not a particularly good approximation for most locations along the survey course in Figure 1. Whether this behavior is representative of other places on Earth will be the subject of a future investigation.

In Figure 12 we also show data for locations between places where we actually calculated apparent cutoffs. For these locations, apparent cutoffs are estimated with a simple spline interpolation of the results shown in Figure 11. In general, the deviation of these points from the Dorman function is also reduced, indicating that the apparent cutoff is, as one might hope, a more or less continuous function of geographical position.

6. Summary

We have defined an "apparent" cutoff that provides a better organization of neutron monitor count rates from a latitude survey than the effective vertical cutoff. Use of the apparent cutoff eliminates most of an anomaly observed in the 6-8 GV region during the 1994-1995 Bartol/Tasmania latitude survey. The FLUKA and HEAVY packages are reasonably accurate at calculating particle propagation through the atmosphere. Our atmospheric model is not complete, and we plan to repeat the analysis with a more accurate representation of the atmosphere, incorporating the Earth's surface curvature and magnetic deflection of the particles, including secondaries, within the atmosphere. We also plan to use FLUKA to calculate a new neutron monitor detection response for comparison with the *Hatton* [1971] data. In addition, we are investigating techniques to permit more rapid calculation of apparent cutoffs.

Acknowledgments. We would like to thank Alfredo Ferrari, Tom Gaisser, and Todor Stanev for allowing the use of their transport libraries and for help with the propagation simulation. We would also like to thank the officers and crew of USCGC *Polar Star* (WAGB-10) for their assistance in conducting this survey. This work was supported by National Science Foundation grants OPP-9528122, ATM-9616619, and OPP-9424005 and by the Australian Research Council.

The Editor thanks J. A. Lockwood and another referee for their assistance in evaluating this paper.

References

Allkofer, O., and P. Grieder, *Cosmic Rays on Earth, Fachinformationszentrum*, Karlsruhe, Germany, 1984.

Beatty, J.J., et al., The cosmic-ray ^{3}He/^{4}He ratio from 100 to 1600 MeV amu^{-1}, *Astrophys. J., 413*, 268, 1993.

Cooke, D.J., J.E. Humble, M.A. Shea, D.F. Smart, N. Lund, I.L. Rasmussen, B. Byrnak, P. Goret, and N. Petrou, On cosmic ray cut-off terminology, *Nuovo Cimento Soc. Ital. Fis. C, 14*, 213, 1991.

Dorman, L.I., S. Fedchenko, L. Granitsky, and G. Rische, Coupling and barometer coefficients for measurements of cosmic ray variations at altitudes of 260-400 mb, *Acta Phys. Acad. Sci. Hung.*, 29 suppl. 2, 233, 1970.

Engel, J., T. Gaisser, P. Lipari and T. Stanev, Nucleus-nucleus collisions and interpretation of cosmic ray cascades, *Phys. Rev. D. Part. Fields, 46*, 5013, 1992.

Fassò, A., A. Ferrari, J. Ranft, P.R. Sala, G.R. Stevenson, and J.M. Zazula, A comparison of FLUKA simulations with measurements of fluence and dose in calorimeter structions, *Nucl. Instrum. Methods Phys. Res., Sect. A, 332*, 459, 1993.

Fassò, A., A. Ferrari, J. Ranft, and P.R. Sala, FLUKA: Present status and future developments, in *Proceedings of the IV International Conference on Calorimetry in High Energy Physics*, p. 493, edited by A. Menzione and A. Scribano, World Sci., River Edge, N.J., 1994.

Fassò, A., A. Ferrari, J. Ranft, and P.R. Sala, FLUKA: Performances and applications in the intermediate energy range, in the proceedings of the Specialists' Meeting on Shielding Aspects of Accelerators, Targets & Irradiation Facilities, p. 287, Organ. for Econ. Dev., Arlington, Tx., 1995.

Fassò, A., A. Ferrari, J. Ranft, and P.R. Sala, An update about FLUKA, in the proceedings of the 2nd workshop on Simulating Accelerator Radiation Environment, Eur. Organ. for Nucl. Res., Geneva, *Div. Rep. CERN/TIS-RP/97-05*, p. 158, 1997.

Gaisser, T., *Cosmic Rays and Particle Physics*, Cambridge Univ. Press, New York, 1990.

Hatton, C.J. *Progress in Elementary Particle and Cosmic Ray Physics*, vol. X, Elsevier New York, 1971.

Lin, Z., J.W. Bieber, and P. Evenson, Electron trajectories in a model magnetosphere: Simulation and observation under active conditions, *J. Geophys. Res., 100*, 23,543, 1995.

Moraal, H., M.S. Potgieter, P.H. Stoker and A.J.van der Walt, Neutron monitor latitude survey of cosmic ray intensity during the 1986/1987 solar minimum, *J. Geophys. Res., 94*, 1459, 1989.

Rao, U.R., K.G. McCraken and D. Venkatesan, Asymptotic cones of acceptance and their use in the study of daily variation of cosmic radiation, *J. of Geophys. Res., 68*, 345, 1963.

Rossi, B., Interpretation of cosmic phenomena, *Rev. Mod. Phy., 20*, 537, 1948

Seo, E., J.F. Ormes, R.E. Streitmatter, S.J. Stochij, W.V. Jones, S.A. Stephens and T. Bowen, Measurement of

galactic cosmic ray proton and helium spectra during the 1987 solar minimum, *Astrophys. J., 378*, 763, 1991.

Shea, M.A., D.F. Smart and K.G. McCraken, A study of vertical cutoff rigidities using sixth degree simulations of the geomagnetic field, *J. Geophys. Res., 70*, 4117, 1965.

Stoker, P.H., Neutron monitor latitude surveys, response functions and 22-year modulation, *Proc. Int. Conf. Cosmic Rays 24th, 4*, 1082, 1995.

Sullivan, J.D., Geometrical factor and directional response of single and multi-element particle telescopes, *Nucl. Instrum. Methods, 95*, 5, 1971.

Zombeck, M., *Handbook of Space Astronomy and Astrophysics*, Cambridge Univ. Press, New York, 1982.

J. W. Bieber ,J. M. Clem and P. Evenson, Bartol Research Institute, University of Delaware, Newark, DE 19716, USA. (e-mail: john@bartol.udel.edu; clem@bartol.udel.edu; penguin@bartol.udel.edu)

D. Hall and J. E. Humble, Department of Physics, University of Tasmania, Hobart, Tasmania, 7001, Australia. (e-mail: John.Humble@utas.edu.au; dhall@denshi.shinshu-u.ac.jp)

M. L. Duldig, Australian Antarctic Division, Kingston, Tasmania 7050, Australia. (e-mail: Marc.Duldig@utas.edu.au)

(Received July 3, 1997; accepted August 13, 1997.)